ADVANCE RESEARCH JOURNAL OF MULTIDISCIPLINARY DISCOVERIES
ISSN : 2456-1045
VOL.37 I ISSUE-1 I CHAPTER-1
PUBLISHER : INTERNATIONAL JOURNAL FOUNDATION (IJF)



# Interaction of Harmonic Waves on A Viscoelastic Cylindrical Shell

*** Safarov Ismoil Ibrokhimovich[1], Kuldashov Nasriddin Urinovich[2], Kulmuratov Nurillo Rakhimovich[3]**

*[1,2]Tashkent Institute of Chemistry and Technology, Tashkent, Republic of Uzbekistan.*
*[3]Navoi state mining institute, Navoi, Republic of Uzbekistan*

**ANNOTATION**

The paper considers the effects of harmonic waves on a spatial cylindrical shell with a liquid. The problem is solved in the mixing potentials. A method of solution and algorithm was developed. The result is a count and an analysis is made.

**Keywords :** shell, liquid, mixing, diffraction, stresses.

**ORIGINAL RESEARCH ARTICLE**

**ISSN :** 2456-1045 (Online)
**(ICV-CHT/Impact Value):** 72.30
**(GIF) Impact Factor:** 5.188
**Publishing Copyright @** International Journal Foundation
**Journal Code:** ARJMD/CHT/V-37.0/I-1/C-1/MAY-2019
**Category :** CHEMICAL TECHNOLOGY
**Volume :** 37.0/**Chapter-** I/**Issue** -1 (MAY-2019)
**Journal Website:** www.journalresearchijf.com
**Paper Received:** 29.03.2019
**Paper Accepted:** 24.05.2019
**Date of Publication:** 05-06-2019
**Page:** 01-10

**Name of the Corresponding author:**

**Safarov Ismoil Ibrokhimovich***

Tashkent Institute of Chemistry and Technology, Tashkent, Republic of Uzbekistan.

**CITATION OF THE ARTICLE**

**Ibrokhimovich SI., Urinovich KN., Rakhimovich KN;** (2019) Interaction of Harmonic Waves on A Viscoelastic Cylindrical Shell; *Advance Research Journal of Multidisciplinary Discoveries;* 37(1) pp. 01-10



## I. INTRODUCTION

Wave effects, reflections, diffraction and interference have a significant impact on the complex stress state of the array arising in the case of several closely located underground structures and located near the free surface. This and other wave effects can be taken into account only by the methods of wave dynamics, where accelerograms can also be used [1], [2], [3], [4]. The present work considers the effect of harmonic waves on a viscoelastic shell located in a viscoelastic medium.

### 1.1 Statement of the problem of interaction of seismic waves cylindrical body with fluid

In this section, the problems of the interaction of non-stationary waves in cylindrical bodies in an elastic medium are solved. Let an elastic N-layer cylinder be placed in an infinite elastic medium containing filler [5]. Non-stationary stress waves $\sigma_{xx}^{(i)}$ and $\sigma_{xy}^{(i)}$ whose fronts are parallel to the longitudinal axis of the cylinder fall on a layered cylinder. The dynamic behaviour of the stress-strain state of a dissipative mechanical system consisting of deformable and non-deformable bodies is considered. The relationship of stresses $\sigma_{ij}$ and strains $\varepsilon_{ij}$ for the elements of the mechanical system satisfies the linear hereditary Boltzmann-Aviary relations, which we take in the form:

$$s_{ij} = 2\sigma(e_{ij} - \int_{-\infty}^{t} R(t-\tau)e_{ij}(\tau)d\tau) \quad \ldots\ldots \quad (1)$$

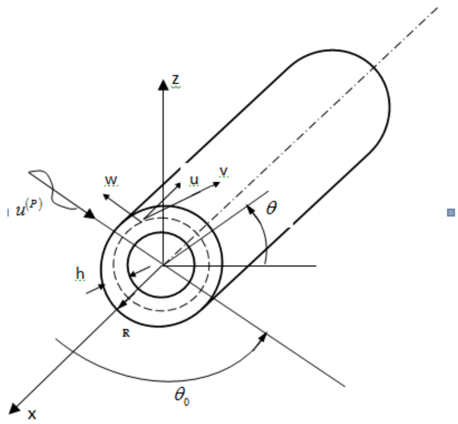


**Fig.1. Effect of elastic waves on a cylindrical shell**

Where, $s_{ij}$ is the stress deviator $\sigma_{ij}$, $e_{ij}$ the deviation deviator $\varepsilon_{ij}$, $\sigma = \sigma_{ij}/3$, $R$ is an R-weakly singular relaxation core, taken in the form

$$R(t) = Ae^{-\beta t} \cdot t^{\alpha-1}, \quad \ldots\ldots\ldots\ldots\ldots\ldots \quad (2)$$

Here, E is the instantaneous modulus of elasticity, A, $\alpha$ and $\beta$ are dimensionless parameters. The parameters of the relaxation core and the instantaneous modulus of elasticity are determined from quasistatic experiments using the method described in [6]. The equations of motion of the deformable layer in the absence of mass forces are:

$$\tilde{\mu}_n \nabla^2 \vec{u} + (\tilde{\lambda}_n + \tilde{\mu}_n) graddi\vartheta\, \vec{u} = \rho_n \frac{\partial^2 \vec{u}}{\partial t^2}, \text{ n =1, 2, 3..N.} \quad \ldots\ldots. \quad (3)$$

$$L\vec{u} - L_0 \int_0^t R_L(t-\tau) L\vec{u}(\tau)\, d\tau = \frac{(1-\nu_0^2)}{E_0 h_0}\vec{p} + \rho_0 \frac{(1-\nu_0^2)}{E_0}\left(\frac{\partial^2 \vec{u}}{\partial t^2}\right),$$

$$\tilde{\lambda}_n \varphi(t) = \lambda_n\left[\varphi(t) - \int_0^t R_\lambda(t-\tau)\varphi(\tau)\, d\tau\right], \tilde{\mu}_n \varphi(t) = \mu_n\left[\varphi(t) - \int_0^t R_\mu(t-\tau)\varphi(\tau)\, d\tau\right]$$

Where $\tilde{\mu}_n, \tilde{\lambda}_n$ is the instantaneous coefficient of the viscoelastic operator;

$R_L, R_\lambda, R_\mu$ - core relaxation;

$\varphi(t)$ - arbitrary functions of time. It is required to determine the dynamic stress-strain state of the cylinder and its environment caused by the incident harmonic stress waves. The interaction of seismic waves with a cylindrical shell is considered (Fig. 1). Let an arbitrary seismic wave act on a cylindrical shell. The equation of motion of the environment and the shell is written in cylindrical coordinates. At the contact of the shells with the medium conditions of hard contact are set, i.e. the condition of equality of displacements and stresses is satisfied. The main goal of solving these problems is to show the influence of the angle of incidence $\theta_0$ on the stress-strain state of the system [7].

### 1.2. Solution methods The problem is solved in the mixing potentials.

Then the displacement vector is represented in the form of potential and solenoid parts, then the displacement of the medium, respectively, have the form

$$\vec{u}_j = grad\phi_j + rot\vec{\psi}_j$$

where $\phi_j$ is the potential of longitudinal waves;

$\vec{\psi}_j(\psi_j, 0, \chi_j)$ - potential of transverse waves.

Displacement vectors, deformations and displacement potentials in cylindrical coordinate systems are expressed as:

$$\nabla^2\phi_j - \frac{1}{c_{pj}^2 \Gamma_{\kappa j}} \frac{\partial^2 \phi_j}{\partial t^2} = 0;$$

$$\nabla^2\psi_j - \frac{1}{c_{Sj}^2 \Gamma_{\kappa j}} \frac{\partial^2 \psi_j}{\partial t^2} = 0,$$

$$\nabla^2\chi_j - \frac{\chi_j}{r^2} + \frac{2}{r^2}\frac{\partial \chi_j}{\partial \theta} - \frac{1}{c_{sj}^2 \Gamma_{\kappa j}} \frac{\partial^2 \chi_j}{\partial t^2} = 0, \quad \ldots\ldots \quad (4)$$

Where $\Gamma_{\kappa j} = 1 - \Gamma_j^C(\omega_R) - i\Gamma_j^S(\omega_R)$ (ω); $c_{pj}^2 = (\lambda_j + 2\mu_j)/\rho_j$; $c_{sj}^2 = \mu_j/\rho_j$ – respectively, the propagation velocity of longitudinal and transverse waves in an elastic body.

The solution of equation (4) with (i = 1) is written as

$$\begin{pmatrix} \phi_1 \\ \psi_1 \\ \chi_1 \end{pmatrix} = \sum_{n=1}^{\infty} \begin{pmatrix} A_{n1} H_n^{(1)}(\gamma_1 r) \\ B_{n1} H_n^{(1)}(\delta_1 r) \\ C_{n1} H_n^{(1)}(\delta_1 r) \end{pmatrix} \begin{pmatrix} \begin{pmatrix} \cos(n\theta) \\ -\sin(n\theta) \end{pmatrix} \\ \begin{pmatrix} \sin(n\theta) \\ \cos(n\theta) \end{pmatrix} \\ \begin{pmatrix} \cos(n\theta) \\ -\sin(n\theta) \end{pmatrix} \end{pmatrix} e^{i\alpha(x-ct)} \quad (5)$$

Where $\gamma_1 = \sqrt{\alpha^2 - K_{p1}^2}$; $\delta_1 = \sqrt{\alpha^2 - K_{s1}^2}$; $K_{p1}^2 = \omega^2 / c_{p1}^2 \bar{\Gamma}_{\kappa 1}$; $K_{s1}^2 = \omega^2 / c_{s1}^2 \hat{\Gamma}_{\kappa 1}$. $A_{n1}C_{n1},B_{n1}$ - arbitrary constants, $H_n^{(1)}$ are Hankel functions of the 1st kind of the nth order. For $i \neq 1$ (5), the following form

$$\begin{pmatrix} \phi_j \\ \psi_j \\ \chi_j \end{pmatrix} = \sum_{n=1}^{\infty} \begin{pmatrix} A_{nj} H_n^{(1)}(\gamma_j r) + M_{nj} H_n^{(2)}(\gamma_j r) \\ B_{nj} H_n^{(1)}(\delta_j r) + D_{nj} H_n^{(2)}(\delta_j r) \\ C_{nj} H_n^{(1)}(\delta_j r) + L_{nj} H_n^{(2)}(\delta_j r) \end{pmatrix} \begin{pmatrix} \begin{pmatrix} \cos(n\theta) \\ -\sin(n\theta) \end{pmatrix} \\ \begin{pmatrix} \sin(n\theta) \\ \cos(n\theta) \end{pmatrix} \\ \begin{pmatrix} \cos(n\theta) \\ -\sin(n\theta) \end{pmatrix} \end{pmatrix} e^{i\alpha(x-ct)} \quad (6)$$

where Anj, Bnj, Cnj, Mnj, Dnj, Lnj are arbitrary constants, which is determined from the boundary conditions, $H_n^{(1)}$ and are Hankel functions of the 1st kind of the n-th order.

The displacement and stress of the elastic medium, taking into account (6), takes the following form:

$$U_{r1} = \sum_{n=0}^{\infty}(A_{n1}K_n`(\gamma_1 r) + B_{n1}\frac{n}{r}K_n(\delta_1 r) + e(i\alpha)C_{n1}K_n`(\delta_1 r)\begin{Bmatrix} \cos n\theta \\ -\sin n\theta \end{Bmatrix} e^{i\alpha(x-ct)}$$

$$U_{\theta 1} = \sum_{n=0}^{\infty}(\frac{n}{r}A_{n1}K_n(\gamma_1 r) - B_{n1}K_n`(\delta_1 r) - \frac{e}{r}i\alpha C_{n1}K_n(\delta_1 r))\begin{Bmatrix} \sin n\theta \\ \cos n\theta \end{Bmatrix} e^{i\alpha(x-ct)} \quad (7)$$

$$U_{z1} = \sum_{n=0}^{\infty}\left\{A_{n1}(i\alpha)K_n(\gamma_1 r) - C_{n1}e(\frac{1}{r}K_n`\delta_1 r) + K_n``(\delta r) - \frac{n^2}{r^2}K_n(\delta r))\right\} \begin{Bmatrix} \cos n\theta \\ -\sin n\theta \end{Bmatrix} e^{i\alpha(x-ct)};$$

$$\delta_{rr1} = \sum_{n=0}^{\infty}\left\{A_{n1}(\lambda_r\left[\frac{1}{r}K_n`(\gamma_1 r) + \frac{n^2}{r^2}K_n(\gamma_1 r) - \alpha^2 K_n(\gamma_1 r)\right] + 2\mu_r K_n``(\gamma r)) + \right.$$

$$\left. + B_{n1}(\lambda_r\frac{n}{r}(1-\frac{1}{r})K_n(\delta_1 r) + 2\mu r\frac{n}{r}K_n`(\delta r) + C_{n1}(\lambda_r\left[(i\alpha e)K_n``(\delta_1 r) - ie(\frac{n^2}{r^2}\alpha + \delta_1^{2)}K_n(\delta_1 r)\right] + 2\mu_\Gamma i\alpha e K_n`(\delta r)\right\} \begin{Bmatrix} \cos n\theta \\ -\sin n\theta \end{Bmatrix} e^{i\alpha(x\pm ct)};$$

$$\delta_{r\theta_1} = \sum_{n=0}^{\infty}\left\{\frac{n}{r}\mu_\Gamma A_{n1}(\frac{1}{r})K_n(\gamma_1 r)K_n`(\gamma_1 r) + \frac{n\mu_\Gamma}{2r}C_{n1}(i\alpha e)(\frac{2}{r}K_n(\delta_1 r) - K_n`(\delta_1 r)\right\} \begin{Bmatrix} \sin n\theta \\ \cos n\theta \end{Bmatrix} e^{i(\omega t \pm \alpha x)};$$

$$\delta_{rX_1} = \sum_{n=0}^{\infty}\left\{A_{n1}\mu_1(ia)K_n(\gamma_1 r) + B_{n1}\frac{ia}{2r}\mu_1 K_n(\delta_1 r) + C_n i(ae - \delta^2)K_n`(\delta_1 r)\right\} \begin{Bmatrix} \sin n\theta \\ \cos n\theta \end{Bmatrix} e^{i(\omega t \pm \alpha x)};$$

We assume that a cylindrical layer (shell) is affected by one of the harmonic supply waves of the type P, SH and SV in the form

$$\begin{pmatrix}\varphi^{(p)}\\ \psi^{(p)}\\ \chi^{(p)}\end{pmatrix}=U_0^{(p)}\begin{pmatrix}\frac{1}{iK_1}\\ \frac{1}{iK_2\sin\theta_0}\\ \frac{1}{iK_2\sin\theta_0}\end{pmatrix}e^{i\alpha(x-ct)}\sum_{n=0}^{\infty}\begin{pmatrix}a_{n1}J_n(\gamma r)\\ b_{n1}J_n(\delta_1 r)\\ C_{n1}J_n(\delta_1 r)\end{pmatrix}\begin{pmatrix}cos n\theta\\ \sin n\theta\\ \sin n\theta\\ \cos n\theta\\ \cos n\theta\\ -\sin n\theta\end{pmatrix} \qquad \text{……………………. (8)}$$

$$\begin{pmatrix}\alpha_{n1}\\ b_{n1}\\ c_{n1}\end{pmatrix}=\begin{cases}1, & n=0\\ 2i^n & n>0\end{cases},\quad \alpha=\begin{cases}K_1\cos\theta_0 & -SP\\ K_2\cos\theta_0 & -SP\ ,\ SH\end{cases}$$

If one of the components of the incident wave is known, then using the known formulas and (7) one can find the environment movements: For example, under the action of the P wave, according to the formula (7) the displacement vector takes the following form:

$$\begin{pmatrix}U_r^{(p)}\\ U_\theta^{(p)}\\ U_x^{(p)}\end{pmatrix}=U_0^{(p)}\begin{bmatrix}1,\\ -r^{-1}\\ i\alpha\end{bmatrix}\frac{1}{iK_1}e^{-\alpha(x-ct)}\sum_{n=0}^{\infty}E_n i^1\begin{bmatrix}J_n^1(\delta_1 r)\\ nJ_n(\delta_1 r)\\ J_n(\delta_1 r)\end{bmatrix}\begin{bmatrix}\cos n\theta\\ \sin n\theta\\ \cos n\theta\\ \sin n\theta\\ \cos n\theta\\ -\sin n\theta\end{bmatrix}$$

Similarly, environmental movements are recorded under the action of SV and SH waves.

$$\sigma_{rr}^{(p)}=U_0^{(p)}\frac{1}{iK_1}e^{i\alpha(\overset{\infty}{x}-ct)}\sum_{n=0}E_n\left[\lambda_2\left(\frac{1}{r}J_n(\gamma r)+J_n(\gamma,r)-\left(\frac{n^2}{r^2}+\alpha^2\right)J_n(\gamma r)\right)+2\mu r J_n(\gamma r)\right]J\cos n\theta \quad \sigma_{r\theta}^{(p)}=-2\mu_r e^{i\alpha(\overset{\infty}{x}-ct)}\frac{U_0^{(p)}}{iK_1}(i\alpha-\frac{1}{r})\sum_{n=0}E_n nJ_n(\gamma r)\sin n\theta,$$

$$\sigma_{rx}^{(p)}=2\mu_r U_0^{(p)}\frac{1}{iK_1}(i\alpha)e^{i\alpha(x-ct)}\sum_{n=0}^{\infty}nE_nJ_n(\gamma r)\sin n\theta; \quad ,$$

We introduce the following notation.

$$S_{1n}=U_0^{(p)}\frac{1}{iK_1}(i\alpha)e^{i\alpha(\overset{\infty}{x}-ct)}\sum_{n=0}nE_nJ_n(\gamma r)+2\mu r_{J_n}^{''}(\gamma r)$$

$$S_{2n}=2\mu_r(i\alpha-\frac{1}{r})E_{n1}nJ_n(\gamma r);\quad S_{3n}=2\mu_r(i\alpha)nE_{n1}J_n(\gamma r),$$

After these designations, the above indicated voltages take the following form:

$$\sigma_{rr}^{(p)}=U_0^{(p)}\frac{1}{iK_1}e^{i\alpha(\overset{\infty}{x}-ct)}\sum_{n=0}^{\infty}S_{1n}\cos n\theta,$$

$$\sigma_{r\theta}^{(p)}=U_0^{(p)}\frac{1}{iK_1}e^{i\alpha(\overset{\infty}{x}-ct)}\sum_{n=0}^{\infty}S_{2n}\sin n\theta \qquad \text{……………. (9)}$$

$$\sigma_{rx}^{(p)}=U_0^{(p)}\frac{1}{iK_1}e^{i\alpha(\overset{\infty}{x}-ct)}\sum_{n=0}^{\infty}S_{3n}\sin n\theta$$

The resulting displacement field and voltage consists of two displacements under the action of incident and reflected waves. The solution for a cylindrical layer (i = 2) is written as:

$$\begin{pmatrix}\varphi_2\\ \varphi_2\\ \varphi_2\end{pmatrix}=\sum_{n=0}^{\infty}\sum_{n=0}^{\infty}\begin{pmatrix}a_{n1}J_n(\gamma_2 r)+B_{n2}N_n(\gamma_2 r)\\ C_{n1}J_n(\delta_2 r)+D_{n2}N_n(\delta_2 r)\\ M_{n2}J_n(\delta_1 r)+K_{n2}N_n(\delta_2 r)\end{pmatrix}\begin{pmatrix}cos n\theta\\ \sin n\theta\\ \sin n\theta\\ \cos n\theta\\ \cos n\theta\\ -\sin n\theta\end{pmatrix}e^{ia(x-ct)} \qquad \text{……………….(10)}$$

where $\gamma_2=\sqrt{K_{p2}^2-\alpha^2}\ \ \delta_2=\sqrt{K_{S2}^2-\alpha^2}\ ,x_{p2}^2=w^2/C_{p2}^2\ \ x_{S2}=\frac{w^2}{C_{S2}^2}$, $J_n$, $N_n$- Bessel function of the 1st and 2nd kind, respectively; $A_{n2}$ $B_{n2}$ $C_{n2}$ $D_{n2}$ $M_{n2}$ and $K_{n2}$ are arbitrary constants which are determined from the condition on the inner surface of the layer and the contact in the following form:

$$r=r_0:\ \sigma_{rr2}=0;\sigma_{r\theta 2}=0;\sigma_{rz2}=0\ ,r=r_1:\ U_{r1}=U_{r2};U_{\theta 1}=U_{\theta 1};U_{z1}=U_{z2};\sigma_{rr1}=\sigma_{rr2};\sigma_{rz1}=\sigma_{rz2} \qquad \text{………… (11)}$$

After substituting the corresponding displacements and stresses into (11), we obtain an inhomogeneous complex system of algebraic equations with 9 unknowns ($A_{n1}$ $B_{n1}$ $C_{n1}$ $A_{n2}$ $B_{n2}$ $C_{n2}$ $D_{n2}$ $M_{n2}$ and $K_{n2}$). If a cylindrical shell is considered in place of a cylindrical layer, then we obtain the following equation of shell motion:

$$\begin{aligned}
&\frac{\partial^2 u}{\partial x^2}+\frac{1-\nu_0}{2R^2}\frac{\partial^2 u}{\partial \theta^2}+\frac{1+\nu_0}{2R}\frac{\partial^2 v}{\partial x \partial \theta}+\frac{\nu_0}{R}\frac{\partial w}{\partial x}-\frac{1-\nu_0}{E_0 h_0}\rho_0\frac{\partial^2 u}{\partial t^2}+P_1=0\\
&\frac{1+\nu_0}{2R}\frac{\partial^2 u}{\partial x \partial \theta}+\frac{1-\nu_0}{2}\frac{\partial^2 v}{\partial x^2}+\frac{1}{R^2}\frac{\partial^2 v}{\partial \theta}+\frac{1}{R^2}\frac{\partial w}{\partial \theta}-\frac{1-\nu_0^2}{E_0 h_0}\rho_0\frac{\partial^2 v}{\partial t^2}+P_2=0 \qquad \ldots\ldots\ldots\ldots\ldots\ldots\ldots\ldots (12)\\
&\frac{\nu_0}{R}\frac{\partial u}{\partial x}+\frac{1}{R^2}\frac{\partial v}{\partial \theta}+\frac{h^2}{12}\left(\frac{\partial^2 w}{\partial x^4}+\frac{2}{R^2}\frac{\partial^4 w}{\partial x^2 \partial \theta^2}+\frac{2}{R^4}\frac{\partial^4 w}{\partial \theta^4}\right)-\frac{1-\nu_0^2}{E_0 h_0}\rho_0\frac{\partial^2 w}{\partial t^2}+P_3=0
\end{aligned}$$

here R is the radius of the middle surface of the shell; $h_0$ is the thickness of the shell;
$E_0$ is Young's modulus; $v_0$ is the Poisson's ratio; $\rho_0$ is the density of the shell material; θ is the angle measured from the initial generator; χ is the distance from the coordinate plane along the generator to the point in question:

$$\begin{pmatrix} P_1 \\ P_2 \\ P_3 \end{pmatrix} = \frac{1-v_0^2}{E_0 \mathrm{h}_0}\begin{pmatrix} \sigma_{r\chi} \\ \sigma_{r\theta} \\ \sigma_{rr} \end{pmatrix}.$$

At the contact boundary, a continuity condition is set:

$$\left.\begin{aligned} U_{r1} &= W - U_r^{(p)} \\ U_{\theta 1} &= V - U_0^{(p)} \\ U_{\chi 1} &= U - U_\chi^{(p)} \end{aligned}\right\}$$

The solution of the system of partial differential equations for thin shells takes the form:

$$\begin{pmatrix} U \\ V \\ W \end{pmatrix} = \sum_{n=0}^{\infty}\begin{pmatrix} U_n^{(1)} \\ V_n^{(1)} \\ W_n^{(1)} \end{pmatrix}\begin{pmatrix} \begin{pmatrix} \cos n\theta \\ -\sin n\theta \end{pmatrix} \\ \begin{pmatrix} \sin n\theta \\ \cos n\theta \end{pmatrix} \\ \begin{pmatrix} \cos n\theta \\ -\sin n\theta \end{pmatrix} \end{pmatrix} e^{ia(x-ct)} \qquad \ldots\ldots\ldots\ldots\ldots\ldots\ldots \quad (13)$$

where Un (1), Vn (1), Wn (1) are arbitrary constants determined by the joint solution of (11) and (12). After substituting (13) into (11) and (12), we obtain the following system of algebraic equations with complex coefficients

1) $$\sum_{n=0}^{\infty}\left[A_{n1}K_n(\gamma R)+B_{n1}\frac{n}{K}K_n(\delta R)+e(ia)C_{n1}K_n(\delta R)\right]\bullet$$
$$\bullet\begin{pmatrix} cosn\theta \\ -\sin n\theta \end{pmatrix} e^{ia(x-ct)}+U_0^{(P)}\frac{1}{iK_1}e^{ia(x-ct)}\sum_{n=0}^{\infty}E_n J_n'(\gamma R)\cos n\theta=\sum_{n=0}^{\infty}W_n^{(1)}\begin{pmatrix} cosn\theta \\ -\sin n\theta \end{pmatrix}e^{ia(x-ct)}$$

2) $$\sum_{n=0}^{\infty}\left[-\frac{n}{r}A_{n1}K_n(\gamma R)+B_{n1}K_n'(\delta R)-\frac{e}{r}(ia)C_{n1}K_n'(\delta R)\right]\bullet$$
$$\bullet\begin{pmatrix} -\sin n\theta \\ cosn\theta \end{pmatrix} e^{ia(x-ct)}-\frac{1}{R}U_0^{(P)}\frac{1}{iK_1}e^{ia(x-ct)}\sum_{n=0}^{\infty}nE_n J_n'(\gamma R)\sin n\theta=\sum_{n=0}^{\infty}V_n^{(1)}\begin{pmatrix} \sin n\theta \\ cosn\theta \end{pmatrix}e^{ia(x-ct)}$$

3) $$\sum_{n=0}^{\infty}\left[A_{n1}(ia)K_n(\gamma R)-C_{n1}e\left(\frac{1}{r}K_n'(\delta R)+K_n'(\delta R)-\frac{n^2}{r^2}K_n(\delta R)\right]\bullet$$
$$\bullet\begin{pmatrix} cosn\theta \\ -\sin n\theta \end{pmatrix} e^{ia(x-ct)}=\sum_{n=0}^{\infty}U_n^{(1)}\begin{pmatrix} cosn\theta \\ -\sin n\theta \end{pmatrix}e^{ia(x-ct)}$$

4) $$\sum_{n=0}^{\infty}\left[-a^2U_n^{(1)}-\frac{1-v_0}{2R^2}U_n^{(1)}+\frac{1-v_0}{2R}ian\mathrm{V}_{n1}^{(1)}+\frac{v_0}{R}iaW_n+\frac{1-v_0^2}{E_0h_0}\rho_0\omega^2U_n^{(1)}\right]\begin{pmatrix} cosn\theta \\ -\sin n\theta \end{pmatrix}e^{ia(x-ct)}$$
$$=\sum_{n=0}^{\infty}A_{n1}\mu_1(ia)K_n(\gamma R)+B_{n1}\frac{ia}{2R}\mu_1K_n(\delta R)+C_n\mu_1 i(ae-\delta^2)K_n'(\delta R)\begin{pmatrix} cosn\theta \\ -\sin n\theta \end{pmatrix}e^{ia(x-ct)}=-\frac{1-v_0^2}{E_0h_0}U_0e^{ia(x-ct)}\sum_{n=0}^{\infty}S_{3n}\cos n\theta$$

 ISSN : 2456-1045 (ONLINE)

5)
$$\sum_{n=0}^{\infty}\left\{\frac{1+v_0}{2R}ian\mathrm{V}_n^{(1)}+\left[\frac{1-v_0}{2}ia^2\frac{n^2}{r^2}+\frac{1+v_0^2}{E_0h_0}\rho_0\omega^2\right]\mathrm{V}_n^{(1)}+\frac{a}{R^2}W_n^{(1)}+\right.$$
$$+\frac{1-v_0^2}{E_0h_0}\left(\frac{n}{R}\mu_rA_{n1}\left(\frac{1}{r}K_n(\gamma R)-K_n'(\gamma R)\right)+\frac{\mu_r}{2}B_{n1}\left(\frac{1}{R}K_n'(\delta R)-\frac{n^2}{r^2}K_n(\delta R)-K_n''(\delta R)\right)+\frac{n\mu^2}{2R}C_{n1}(iae)\left(\frac{2}{R}K_n(\delta R)-\right.\right.$$
$$\left.\left.-K_n'(\delta R)\right)\right\}\begin{pmatrix}\sin n\theta\\ cosn\theta\end{pmatrix}=\frac{1-v_0^2}{E_0h_0}U_0^{(p)}\frac{1}{iK_{(1)}}e^{ia(x-ct)}\sum_{n=0}^{\infty}S_{2n}\sin n\theta$$

6)
$$\sum_{n=0}^{\infty}\left\{ia\frac{v_0}{R}U_0^{(1)}+\frac{n}{R^2}V_n^{(1)}+\left(\frac{h^2}{R}\left(a^4+\frac{2}{R^2}a^2+\frac{n}{R^4}\right)-\frac{1-v_0^2}{E_0h_0}\rho_0\omega^2\right)W_n^{(1)}+\frac{1-v_0^2}{E_0h_0}+\right.$$
$$+\left(A_{n1}\left(\lambda\left(\frac{1}{R}K_n(\gamma R)+\frac{n^2}{R^2}K_n(\delta R)-a^2K_n(\delta R)\right)+2\mu_1K_n''(\gamma R)\right)+B_{n1}\left(\lambda\left(\frac{n}{R}\left(1-\frac{1}{R}\right)K_n(\delta R)+2\mu_1\frac{n}{R}K_n'(\delta R)\right)+\right.\right.$$
$$\left.+C_{n1}\left(\lambda\left((iae)K_n''(\delta R)-ie\left(\frac{n^2}{R^2}a+\delta^2\right)K_n(\delta R)\right)+2\mu_1ieaK_n'(\delta R)\right\}\begin{pmatrix}cosn\theta\\ \sin n\theta\end{pmatrix}e^{ia(x-ct)}=$$
$$=\frac{1-v_0^2}{E_0h_0}U_0^{(p)}\frac{1}{iK_{(1)}}e^{ia(x-ct)}\sum_{n=0}^{\infty}S_{2n}\sin\cos n\theta$$

The main purpose of this work is to compare the annular and axial forces of the shell. Axial and annular forces denote respectively $S_{xx}$ $u$ $S_{ee}$

$$\left.\begin{aligned}S_{xx}&=\left[ciaU+\frac{cv_0}{R}\left(w+\frac{\partial v}{\partial\theta}\right)\right]\begin{pmatrix}\cos n\theta\\-\sin n\theta\end{pmatrix}e^{i(ax-wt)}\\ S_{\theta\theta}&=\left[ciav_0U+\frac{c}{R}\left(w+\frac{\partial v}{\partial\theta}\right)\right]\begin{pmatrix}\sin n\theta\\ \cos n\theta\end{pmatrix}e^{i(ax-wt)}\end{aligned}\right\}\quad\ldots\ldots\ldots\ (14)$$

Where $c=E_0\ h_0/(1-v_0^2)$

Thus, we obtain a complex system of inhomogeneous algebraic equations, which is solved by the Gauss method. In the next section, the results obtained.

## II. DISCUSSION OF NUMERICAL RESULTS

The system of algebraic equations (13) is solved by the Gauss method with the selection of the main element. An algorithm and a program on a computer are compiled to determine the displacement and stress of the shell and the environment under the action of P .SV and SH waves. All results for $\sigma_{xx}$ and $\sigma_{\theta}$ , are obtained as a result of a longitudinal wave (voltage) drop, which is normalized with respect to $\sigma_0^{(p)}(t\to\infty)$

$$\tilde{\sigma}_{xx}=\frac{\sigma_{xx}/h}{\sigma_0^{(p)}}=\frac{E/\rho C_1}{I-v^2}\left[\frac{M^2v^2h}{24(M+Nm)}+\cos\theta^2\frac{M(1-v)+N_1m(1-v^2)}{M+N_1\cdot m}-\ldots\ldots\ldots\ldots\ldots\ (15)\right.$$
$$\left.-\frac{v\cdot M\cdot t^2\sin^2\theta\cdot\cos2\cdot\theta}{M\cdot(\tau^2-1)+N_1\cdot m(2\cdot\tau^2-1)}\right]$$
$$\tilde{\sigma}_{\theta\theta}=\frac{\sigma_{\theta\theta x}/h}{\sigma_0^{(p)}}=\frac{E/\rho C^2}{I-v^2}\left[\frac{M^2t^2}{2\cdot(M+N_im)}+\cos\theta^2\frac{M(1-v)}{M-m\cdot N}-\quad\ldots\ldots\ldots\ldots\ldots\ldots\ldots\ldots(16)\right.$$
$$\left.-\frac{M\cdot t^2\sin^2\theta\cdot\cos2\cdot\theta}{M\cdot(\tau^2-1)+N_1\cdot m(2\cdot\tau^2-1)}\right]$$

Where $M=\mu/G$ From equations (15) and (16) it can be seen that the maximum voltage occurs when $\Theta=\pm\pi/2$. All results are obtained with the following initial data

a) Steel shell in stone $\rho^*=3{,}0$, $\tau=0{,}25, v=0.25\mu=0{,}3;$
b) Concrete shell in solid ground $\rho^*=0{,}84,\tau=0.25,M=0.45,v=0.2;$
c) Concrete shell in soft ground $\rho^*=0{,}84,\tau=0.45,M=0.4,v=0.2;$

In the present work $\mu/\mu_0$ varies in the range of 0.01 <M <1.M = h / R for all cases is 0.05.The numerical results presented below show the importance of the parameter M. The results show (Fig. 2, 3) that the dimensionless ring stress increases with increasing and at the same time the axial stress decreases. In this case, the annular stress is greater than the axial stress in soft ground. This can be seen from formula (16) when

$$\frac{M(1-v)+N\cdot m(1-v^2)}{M+N\cdot m} > \frac{M\cdot\tau^2\cdot v}{M\cdot(\tau^2-1)+N\cdot m(2\cdot\tau^2-1)} \quad \text{......................(17)}$$

Then the maximum value is $\sigma_{xx}$ in $\theta_0 = 0$.

Practice confirms this statement. From formula (16), it can be seen that $\sigma_\Theta$ increases with increasing $\Theta$. If condition (17) is satisfied, then $\sigma_{\theta\theta} > \sigma_{xx}$ for all, provided that $\theta_0$

$$\tau^2 > 4 + \frac{2\cdot N\cdot m(1\pm v)}{M} \quad \text{.......................... (18)}$$

Since $\tau^2$ it is more for soft ground, this condition shows that the circumferential stress is greater than the axial stress for the longitudinal incident wave in soft ground.

**The next task is to study the SH waves.** Moving the environment in this case:

$$u_x^{(p)} = u_y^{(p)} = 0\ , u_z^{(p)} = u_\theta \cdot e^{i\cdot k_2\cdot(x-c_2\cdot t)} \quad \text{................ (19)}$$

Where $c = c_2/\cos\theta_0$ is the speed of the wave in the shell. In our case $c_1 > c > c_2$ it depends on $\theta_0$

$$\sigma_{zx}^{(p)} = -i\cdot u_0^{(p)}\mu\cdot K_2\cdot e^{i\cdot k_2\cdot(x-c_2\cdot t)}$$

Numerical results for $\sigma_{xx}^*$ and $\sigma_{\theta\theta}^*$ normalized to $\sigma_{zx}^{(p)}$. In $n=2$ $\sigma_{xx}^*$ and $\sigma_{\theta\theta}^*$ takes the following form

$$\delta_{\chi\chi}^* = \frac{(E/\rho)\cdot c^2}{1-v^2}\,\frac{v\cdot M\cdot\tau^2\cdot\sin\theta_0\cdot\sin 2\theta_0}{M\cdot(\tau^2-1)+N\cdot m\cdot(2\cdot\tau^2-1)};\ \delta_{\theta\theta}^* = \frac{1}{v}\cdot\delta_{\chi\chi}^* \quad \text{.................. (20)}$$

Fig.4.5 shows the results of the above three cases. In this case, the maximum amplitude appears at $\Theta = \pm\pi/4; \pm 3\pi/4$. From the obtained results it can be seen that under the action of the SV wave the predominant voltage is the ring voltage. They are significantly higher than the rest, if the shell is in soft ground. Let the SH wave fall in the underground shell, in which the potential of the incident waves is determined by the equation

$$\left.\begin{aligned} u_\chi^{(p)} &= -\sin\Theta_0\cdot u_0^{(p)}\cdot e^{i\cdot k_2(\chi-c_2\cdot t)} \\ u_y^{(p)} &= i\cos\Theta_0\cdot u_0^{(p)}\cdot e^{i\cdot k_2(\chi-c_2\cdot t)} \\ u_z^{(p)} &= 0 \end{aligned}\right\} \quad \text{......................... (21)}$$

It is seen that when $\Theta_0 = \pi/2$ the displacements are parallel to the x-axis, $\Theta_0^0 = 0$ and when they are parallel to the y-axis. Tangential stress is determined by the following expression

$$\tau_{xy}^{(p)} = -(\mu_0)\cdot u_0^{(p)}\cdot K_2 \quad \text{........................(22)}$$

Then the normalized axial and annular stresses take the following form:

$$\delta_{xx}^* = \frac{(E/\rho)\cdot C_2^2}{2\cdot(1-v^{2)}}\cdot\sin 2\cdot\Theta_0\cdot\left[\frac{M\cdot(1-v)+N\cdot m(1-v^2)}{M+N\cdot m}+\frac{v\cdot m\cdot\tau^2}{M\cdot(\tau^2-1)+N\cdot m(2\cdot\tau^2-1)}\right] \quad \text{.................. (23)}$$

$$\delta_{\Theta\Theta}^* = \frac{(E/\rho)\cdot C_2^2}{2\cdot(1-v^2)}\cdot\sin\Theta_0\cdot\left[\frac{M\cdot(1-v^2)}{M+N}+\frac{m\cdot\tau^2}{M\cdot(\tau^2-1)+N\cdot m(2\cdot\tau^2-1)}\right] \quad \text{.............................(24)}$$

From the formula (23) $\sigma_{\theta\theta}$ and $\sigma_{xx}$ (24) it is clear that it takes the maximum value at $\Theta_0 = 45^0$. Also $\sigma_{\theta\theta} > \sigma_{xx}$ provided

$$\frac{M\cdot\tau^2}{M(\tau^2-1)+N\cdot m(2\cdot\tau^2-1)} \rangle \frac{N\cdot m(1+v)}{M+N\cdot m}$$

Values $\sigma_{\theta\theta}$ and $\sigma_{xx}$ for options are listed in the table. Figures 6, 7, 8, 9 show $\sigma^*_{xx}$ and $\sigma^*_{\theta\theta}$ the dependences on the frequency Ω, when $\Theta_0 = 5^0$ and 90⁰. It can be seen that in the third case both voltages depend on the frequency a little more than in the first two cases, especially at small angles of incidence. In all these cases, they increase with increasing frequency. Figure 10 shows the variations of voltage versus frequency. From these figures it can be seen that in the first two cases the induced stresses, except for the axial, at small angles of incidence almost do not depend on frequency.

Comparison of the results for two shear waves with longitudinal waves shows that at small angles of incidence on the pipeline (shell), longitudinal waves produce greater stresses than two shear waves. At angles of incidence $\Theta_0 \rangle 90^0$ SV waves Cause more stress than longitudinal. On the other hand, the largest axial stresses are caused by $\Theta_0 = 45^0$. SH waves. In fact, the maximum stress caused in a concrete shell lying in soft ground is due to SH waves, which is much larger than P and SV waves combined.

The tense, deformed state of the environment, caused by the incident of three types of waves, is different. For SV waves, the circumferential stress is greater than the axial stress at 0 in all three cases. For longitudinal waves, on the other hand, the axial stress is greater than the circumferential stress in the first two cases and they depend on the angle of incidence in the third case, despite the fact that the circumferential stress is always greater than the axial stress.

For SH of an incident wave, the circumferential voltage is greater than in the first two examples, but it is less than in the third example (see figure 11).

In this section, we gave a three-dimensional analysis of deep-laid cylindrical shells (pipelines) under the action of seismic waves. Here, at low frequencies, we have obtained simple expressions that can be used to estimate the amplitude of stresses in deep-laid pipelines at a wavelength $\Omega = wR/C_2$

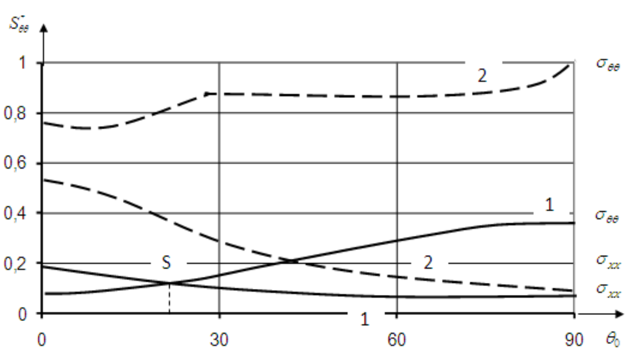

**Fig.2. The dependence of the effort on the angle: 1 and 2 - 1 and 2 group of initial data.**

It is shown that the induced maximum stresses are controlled by the directions of the incident waves and mainly by the coefficient of elasticity of the soil and the shell. This analysis shows that it is important to take spatial factors into account when calculating underground structures. In addition to the above, the amplitude-frequency (ring loads $A_0$) shell characteristic (concrete shell in $\theta = \frac{\pi}{2}, \theta_0 = 90^0$ soft ground) under the action of longitudinal waves was investigated. The results of the calculations are presented in Figure 12, 13, 14, 15, 16. The results show that under the action of seismic waves for underground structures, resonance phenomena can occur.

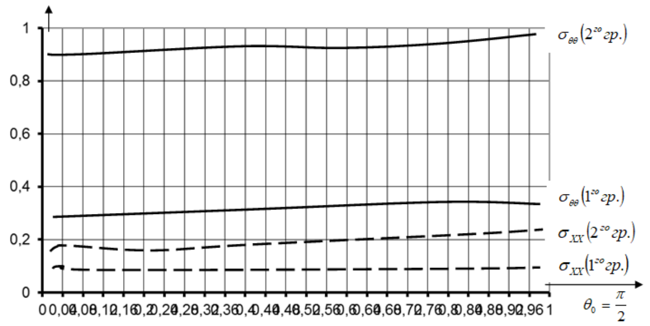

**Fig.3. Change in the annular and axial shells stress at the 3-wave de-activation.**

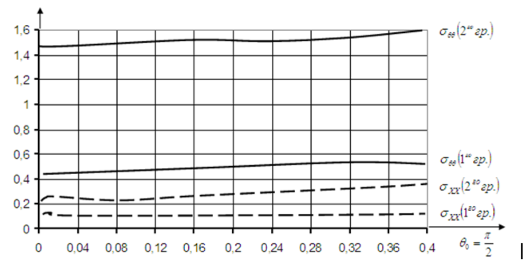

**Fig. 4. The change in the annular and axial shells under the action of the P wave.**

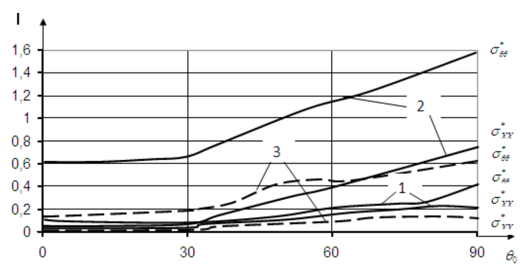

**Fig. 5. The dependence of the ring voltage on the angle: 1 and 2 - 1 and 2 groups of source data; 3 - (the others correspond to the I-th group of initial data) .2**

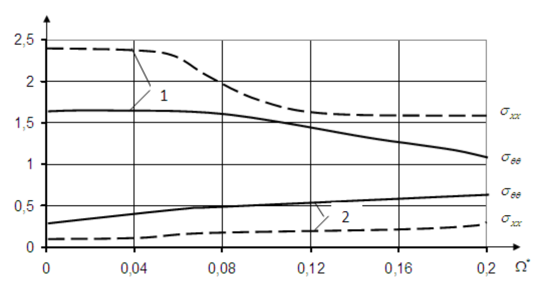

ISSN : 2456-1045 (ONLINE)

**Fig.6. The change in ring and axial stresses as a function of the SH wave.**

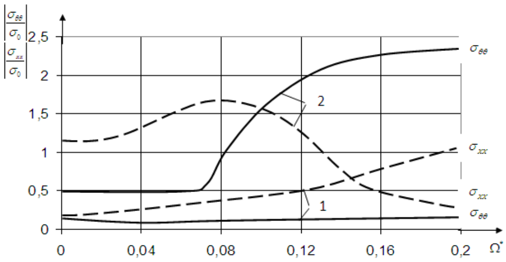


**Fig.7. The change in ring and axial stresses as a function of the SH wave.**

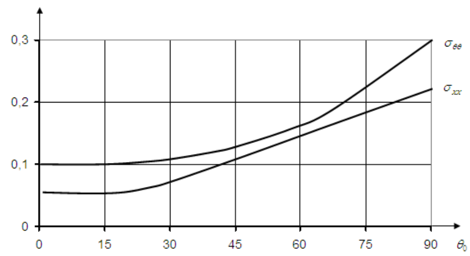


**Fig.8. The dependence of the maximum voltage on the angle of incidence.**
**SV waves. Steel pipe in the ground.**

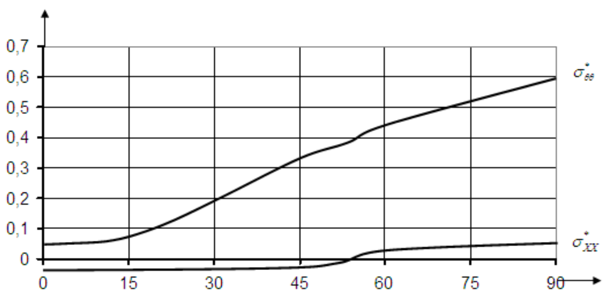


**Fig. 9. The dependence of the maximum voltage on the angle of incidence. SV waves. Concrete pipe in solid ground.**

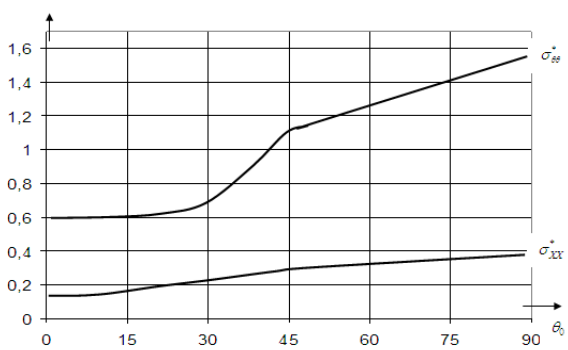


**Fig. 10. The dependence of the maximum voltage on the angle of incidence.**
**SV waves. Concrete pipe in soft ground.**
$\rho = 0{,}84;\ \sigma = 0{,}45;\ m = 0{,}04;\ \nu = 0{,}2;$

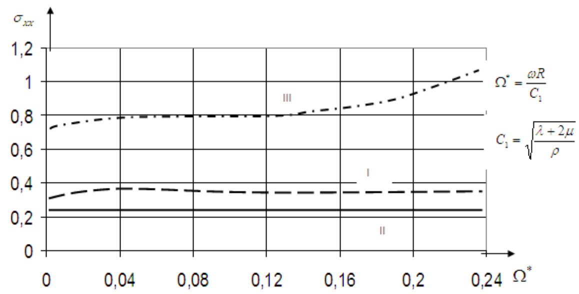


**Fig.11. Maximum amplitude of axial stress versus frequency $\Omega^*\left(\theta_0 = 5^0\right)$.**

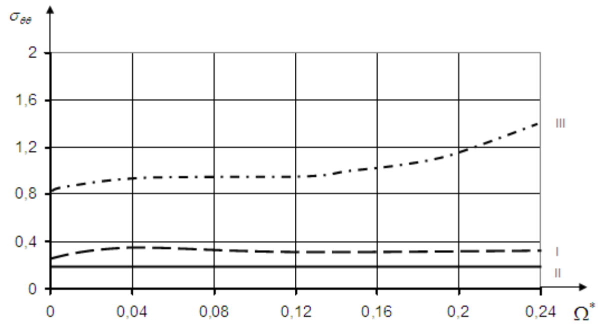


**Fig. 12. Maximum amplitude of ring voltage as a function of frequency $\Omega^*\left(\theta_0 = 5^0\right)$**

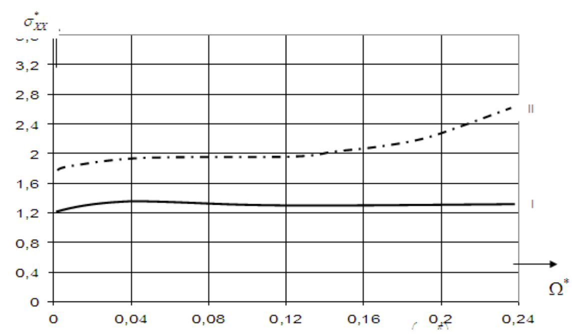


**Fig. 13. The maximum amplitude of the axial stress depending on the frequency P of the wave волны** $\left(\theta_0 = \frac{\pi}{2}\right)$.

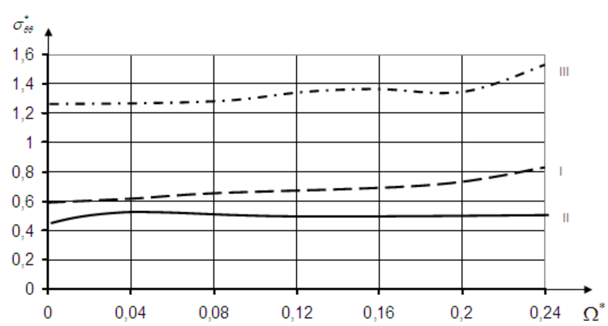


**Fig.14. The maximum amplitude of the ring voltage, depending on the frequency P of the wave** $\left(\theta_0 = \frac{\pi}{2}\right)$.

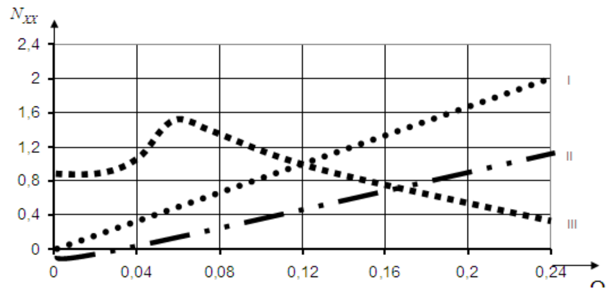


**Fig.15. The maximum amplitude of the axial stress versus the SH frequency of the incident wave in degrees relative to the axis.**

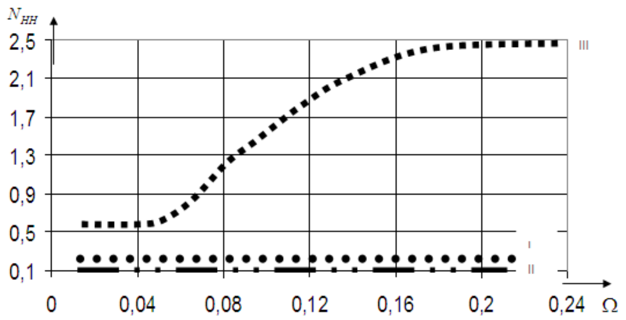


**Fig.16. Maximum amplitude of circumferential voltage depending on frequency (SH wave)**

## III. LITERATURE


[1] **Safarov I.I.** Collisions and waves in dissipatedly non-fertile environments and constructions. - Toshkent. Fan, 1992-250s.

[2] **Koltunov M.A.** Creep and relaxation. M .: Higher School, 1976. 277 p.

[3] **Safarov I.I., Akhmedov M. Umarov A.** Own vibrations of toroidal shell with flowing liquid. Lambert Academic Publishing (Germany). 2017. 177p. hhtp: // dnb. d –nb.de.

[4] **Safarov I.I., Akhmedov M. Sh.,** Buronov S.Method finite elements in the calculations of pipelines. Lambert Academic Publishing (Germany). 2017. 225p. hhtp: // dnb.d –nb.de.

[5] **Safarov I.I., Teshaev M.Kh., Boltaev Z.I.** Distribution of harmonic waves in expansion plastic and cylindrical viscoelastic bodies. Open Science Publishing Raleigh, North Carolina, USA 2017. 218p.

[6] **Mau Mente.** Dynamic stresses and displacement in the vicinity of a cylindrical discontinuity surface from a plane harmonic shear wave. // Applied mechanics, translated from English, vol.30, ser E, No. 3, 1963. p. 117-126.

[7] **Safarov I.I., Boltaev Z.I., Akhmedov M.Sh. Rajabov O.**Numerical number of non-stationary waves by a cylindrical body // Discover 2017.50, (256). April P.255-265. www.discoveryjournals.com


******